Long term friction: from stick-slip to stable sliding

Christophe Voisin, François Renard, Jean-Robert Grasso

Long Term Friction: from Stick-Slip to Stable Sliding

Christophe Voisin[1], François Renard[1,2] and Jean-Robert Grasso[1]

[1]Laboratoire de Géophysique Interne et Tectonophysique, CNRS, Observatoire de Grenoble, Université Joseph Fourier, France

[2] Physics of Geological Processes, University of Oslo, Norway

Abstract. We have devised an original laboratory experiment where we investigate the frictional behaviour of a single crystal salt slider over a large number of deformation cycles. Because of its physical properties, salt, an analogue for natural faults, allows for frictional processes plastic deformation and pressure solution creep to operate on the same timescale. During the same experiment, we observe a continuous change of the frictional behaviour of the slider under constant conditions of stiffness, temperature and loading velocity. The stick-slip regime is progressively vanishing, eventually reaching the stable sliding regime. Concomitantly, the contact interface, observed under the microscope, develops a striated morphology with contact asperities increase in length and width, arguing for an increase in the critical slip distance d_c. Complementary experiments including velocity jumps show that the frictional parameters of the rate and state friction law, a and b, progressively vanish with accumulated slip. The ultimate stage of friction is therefore rate and state independent under our experimental conditions.

1. Introduction

Macroscopic solid friction obeys simple empirical laws, known as Amontons-Coulomb friction laws [*Amontons*, 1699; *Coulomb*, 1785]. They state the existence of a static threshold in friction and that friction depends on the normal load and not on

the apparent contact surface area. Secondary effects have been reported since these laws were first proposed. At rest, the static friction coefficient μ_s increases with the logarithm of time [*Dieterich*, 1972]. This increase is contemporary to the plastic deformation of microscopic contact asperities under stress [*Dieterich and Kilgore*, 1994]. When sliding has begun, friction drops to a dynamic level μ_d, which value is governed by the loading velocity and the material properties. The most complete description of friction is encapsulated in the empirical rate and state friction laws [*Dieterich*, 1979; *Rice*, 1983; *Ruina*, 1983]. These laws stipulate that friction depends on the slip velocity through two parameters a and b; and on a state variable θ that accounts for a mean-field description of memory effects of the interface:

$$\mu=\mu_0+ a\, ln\, (V/V_0) + b\, ln(V\, \theta/d_c),$$

where μ_0 is a reference friction at V_0; V_0 is a reference velocity; V is the slider velocity; d_c is a critical slip distance, akin to the mean size of asperities for instance. Experimental studies have shown the existence of a stable (a-b positive) and an unstable (a-b negative) sliding regime, the latter known as the stick-slip mode. The observation of one or other of these modes is reported to depend on the stiffness of the experimental apparatus and on the loading velocity [*Dieterich*, 1978, 1979; *Heslot et al.*, 1994; *Marone*, 1998; *Shimamoto*, 1986]. As noticed by [*Shimamoto and Logan*, 1984], most of the empirical friction laws are based on short-term experiments and their extrapolation to the geological time scale (long term) is highly speculative because ductile processes (e.g. slow relaxation, pressure-solution, stress corrosion) are active within the upper crust [e.g. *Gratier et al.*, 1999].

In the following, we present results from friction experiments, original in two ways: (i) we use a monocrystal of salt, both brittle and ductile at the laboratory timescale; (ii) the evolving contact interface is observed under the microscope during deformation.

We first describe the experimental apparatus. Second, we report on observations of a continuous change from stick-slip to stable sliding as slip accumulates under constant conditions of sliding velocity, normal load and temperature. Third, we show that the microstructure of the contact interface evolves from randomly rough to some striated morphology. This process of ageing, not observed in plastic or elastic multicontact friction experiments, is driven in our experiments by salt pressure solution creep (PSC). Complementary friction experiments show that the frictional parameters *a* and *b* are decreasing as the slip cumulates. Finally, we propose a physical interpretation to the transition from unstable to stable slip as controlled by the physico-chemical ageing of the initially rough sliding surface.

2. Experimental Method

A cleaved monocrystal of halite (NaCl), roughened with sandpaper, is held under constant normal load and let in contact with a glass window (Figure 1). Salt is used because (i) it is transparent and allows for a direct observation of the contact interface; (ii) it behaves both in a brittle and a ductile way at low stress at ambient temperature and humidity [*Shimamoto*, 1986]; (iii) the plastic deformations are effective over the duration of the friction experiments. Using a salt slider allows for the brittle and ductile deformation to be effective on the time scale of our experiments, aimed to serve as an analogue for natural faults deforming in the brittle and ductile regimes.

The salt slider is mounted on an inverted microscope in order to observe the contact interface. Since halite is transparent, we image the contact asperities at the sliding surface using a high resolution camera located below the halite sample and focused at the slider interface undergoing shear. Doing so, we are able to track any visible deformation at the sliding surface. The slider is subjected to a constant normal load (1186,1g or 2651,4g) and is in contact with a glass or PMMA flat surface. Five

displacement encoders record the plate movement in horizontal and vertical directions (LE/12/S IP50, Solartron). A force sensor (AEP TCA 5kg) records the shear force exerted to move the slider (Figure 1). For all experiments the interface is subjected to ambient humidity. Under these conditions, a thin layer of water is adsorbed on the salt that promotes dissolution-crystallization reactions [*Foster and Ewing*, 2000]. A first set of experiments is conducted at constant velocity. A second set of experiments imposes velocity jumps to the slider in order to estimate the frictional parameters *a* and *b*. All experiments are gouge-free, conducted with bare roughened salt sliders.

3. A Continuous Change from Stick-slip to Stable Sliding

3.1 Changes in the Frictional Behaviour of the Slider

Figure 2A plots the continuous variation in slip of a salt slider against glass, from stick-slip to stable sliding over several hundreds of deformation cycles. At the beginning of the experiment, the slider experiences regular stick-slip oscillations with 35 µm amplitude and 300 s waiting time (Figure 2B). The amplitude and waiting time gradually decrease as the slider enters the episodic stable sliding regime (Figure 2C, 2D and 3A). The waiting time decreases from 300 s to 60 s after 500 cycles, while the slip amplitude decreases from 35 µm to 10 µm. Most of this change occurs during the first 100 cycles. The process continues even when the stick-slip regime has disappeared and once the episodic stable sliding regime is established, with a decreasing period from 60 to 50 s and slip amplitude decreasing from 10 to 8 µm.

The robustness of this change of frictional behaviour is tested with series of experiments conducted with different imposed velocity, initial roughness, and different materials in contact (see auxiliary materials).

3.2 Changes in the Contact Interface Roughness

The change from stick-slip to stable sliding is concomitant with the ageing of the contact interface. The roughness of the slider surface is measured before and after the experiment using white light interferometry (Figure 2A – colour insets). Initially, the surface root mean square (rms) of the roughness is close to 13.40 $\pm$ 0.05 μm. Contact asperities are separated by grooves caused by the roughening process. Their mean size in width and length is about 30 μm. This initial surface is representative of a multicontact interface [*Baumberger and Caroli*, 2006]. By the end of the experiment, for a cumulated slip of 0.6 cm, the sliding surface exhibits a roughness rms of 7.80 $\pm$ 0.05 μm. Contact asperities have grown and adopted an elongated shape in the direction of slip of dimensions 0.5 by 0.2 mm, giving the interface a striated morphology (Figure 2A – colour insets). The drastic change in surface morphology is accompanied by a downward vertical displacement of the slider. Inset in Figure 3 plots the power law relaxation of the vertical displacement with time. It is consistent with a deformation by pressure solution creep of the interface [*Dysthe et al.*, 2002]. The emergence of a strongly anisotropic morphology cannot be explained by the elasto-plastic ageing of the contact interface that leads to an isotropic growth of the contact asperities [*Berthoud et al.*, 1999; *Dieterich and Kilgore*, 1994]. The observed anisotropy arises from the coupling of pressure solution creep and horizontal displacement. Indeed, the change in topography is related to the development of the striated morphology of the contact interface. The matter dissolved from each contact area precipitates in the stress shadow of each asperity, leading to the observed anisotropic pattern.

3.3 Changes in Frictional Parameters *a* and *b*

The two parameters a and b measure the velocity dependence of friction and the increase of static friction with hold time [*Dieterich*, 1979]. The difference (b-a) whenever positive implies a velocity weakening behavior, leading to stick-slip as observed at the beginning of our experiments. We conducted a series of experiments with velocity cycles (jumps from 1 to 10 µm/s) in order to measure these secondary effects of friction. Figure 3B plots three measures of a and b, for different cumulated slips. Both parameters are markedly decreasing with the cumulated slip. After a few centimeters of slip, the velocity jumps are hardly noticeable in the frictional behavior. During this final stage, the change in friction with velocity, if any, is insignificant. Therefore we cannot resolve whether the (b-a) difference changes sign. The slider has evolved from velocity weakening to velocity neutral.

Velocity stepping experiments may be used to infer the value of d_c [*Dieterich*, 1979; *Dieterich and Kilgore*, 1994]: it is defined as the width of the direct friction effect pulse. In the experiment presented in Figure 3B, the estimate of d_c gives a 22.34±5.86 µm, in accordance with the mean size of asperities of the initial contact interface. However, because the direct friction effect disappear after some accumulated slip, the measure of d_c is no more possible. We have to rely on the direct observation of the contact interface and on the mean size of contact asperities as a proxy to d_c.

4. Interpretation

Stick-slip and episodic stable sliding modes are described in the rate and state friction framework [*Dieterich*, 1979]. At constant driving velocity, the occurrence of one or other of these two frictional behaviors is related to a simple condition on the stiffness K of the experimental apparatus [*Heslot et al.*, 1994; *Scholz*, 2002]. To ensure stick-slip oscillations, one must have first $a < b$; second, K must obey the following relation:

147 $$K < K_c = W^*(b\text{-}a)/d_c \quad (1)$$

148 W stands for the normal load exerted on the slider, including its own mass. d_c stands
149 for a length scale typical of the interface, e. g. the mean size of asperities. Equation (1)
150 arises from a stability analysis of a slider block under rate and state friction law [*Rice*
151 *and Ruina*, 1983] and defines the value of the critical stiffness K_c below which stick-
152 slip oscillations do exist. Changes from stick-slip to episodic stable sliding are
153 reported in various conditions. Changes in the driving velocity, in the stiffness or in
154 the normal load all affect the frictional behavior [*Heslot et al.*, 1994]. The presence of
155 a developed gouge also affects the occurrence of stick-slip or stable sliding by
156 changing the (b-a) value [*Beeler et al.*, 1996; *Marone et al.*, 1990]. Finally,
157 temperature changes also affect the value of (b-a) [*Scholz*, 1998].

158 Our experiments are conducted under constant conditions of velocity, mass,
159 stiffness and temperature. The low velocities we use preclude the wear of the slider
160 and the development of a gouge. We must seek for other explanations to the observed
161 transition from stick-slip to stable sliding. Since the normal load W is kept constant
162 throughout the experiments, Equation (1) implies that K_c has to decrease in order to
163 explain the observed change from stick-slip to stable sliding. Our two observations,
164 namely (i) the (b-a) decrease with time and (ii) the contact asperity size increase with
165 time, both contribute to such a K_c decrease with the accumulated slip. The direct
166 observation of topography changes on the frictional interface (Figure 2A), akin to the
167 growth of contact asperities, supports an increase in d_c with time, that is a decrease in
168 K_c. This increase in d_c also implies a stabilization of the slider because of its finite
169 size. Indeed, as d_c increases the nucleation length increases as well, presumably up to
170 the stability limit [*Dascalu et al.*, 2000; *Voisin et al.*, 2002]. In the conditions of the
171 experiment, the increase in d_c is related to changes in the geometry of contact

asperities, the latter being driven by PSC. This mechanism is solely responsible for a fast evolution of the interface under the low normal and shear stress conditions of our experiments [*Gratier*, 1993; *Karcz et al.*, 2006].

Although our experiments are performed under constant conditions of temperature and normal stress, and with no gouge, changes in (b-a) do occur. Indeed, the value of (b-a) approaches zero as both a and b vanish. The immediate consequence is that $K_c \rightarrow 0$ as slip accumulates. Since $(b\text{-}a)=\partial\mu/\partial(\ln V)$, the ultimate frictional behavior of the salt slider is rate independent (Figure 4). A second consequence arises from the definition of b: $b=\partial\mu/\partial \log t$. Since $b\rightarrow 0$ as the slip cumulates, it implies that μ does not increase anymore at rest. The ultimate frictional behavior of the salt slider is state independent.

We explain the change from stick-slip to stable sliding as a progressive decrease in K_c with the cumulative slip. Changing the stiffness of the experiment K will not preclude this evolution to occur. Indeed since $K_c \rightarrow 0$ with the cumulative slip, the change from stick-slip to stable sliding would be observed whatever the stiffness of the experiment. This hypothesis will be the concern of a future work.

5. Conclusion

The frictional behaviour of a single crystal salt slider is investigated under constant conditions of normal load, driving velocity, and temperature. We observe a progressive change from stick-slip to stable sliding with accumulative displacement. During the experiment, all frictional parameters are evolving: a and b are decreasing while d_c is increasing. These changes are contemporary to the morphological evolution of the contact interface, i.e. the development of a striated pattern driven by the coupling of PSC and slip. The increase in d_c and the decrease in (b-a) both lead to the

196 progressive vanishing of K_c, the critical stiffness for stick-slip. The salt slider is
197 therefore forced to a mode of stable sliding, with no more rate and state dependence.
198

199 **Acknowledgments:** We thank P. Giroux, R. Guiguet, and L. Jenatton for their help in designing the
200 experiment; D. Dysthe, J. Feder, D. Brito, J.-P. Gratier, L. Margerin, I. Manighetti , A. Helmstetter, K.
201 Mair for thoughtful discussions. We acknowledge grants from CNRS (ATI, Dyeti) and from Université
202 Joseph Fourier (BQR).
203

204 **References**

205 Amontons, G. (1699), De la résistance causée dans les machines, *Mem. Acad. Roy.*
206 *Sci.*, 206-226.
207 Baumberger, T., and C. Caroli (2006), Solid friction from stick-slip down to pinning
208 and aging, *Advances in Physics*, *55*(3-4), 279-348.
209 Beeler, N. M., et al. (1996), Frictional behavior of large displacement experimental
210 faults, *Journal of Geophysical Research-Solid Earth*, *101*(B4), 8697-8715.
211 Berthoud, P., et al. (1999), Physical analysis of the state- and rate-dependent friction
212 law: Static friction, *Physical Review B*, *59*(22), 14313-14327.
213 Coulomb, C. A. (1785), Théorie des machines simples, *Mém. Math. Phys. Acad. Sci.*,
214 *10*, 161-331.
215 Dascalu, C., et al. (2000), Fault finiteness and initiation of dynamic shear instability,
216 *Earth and Planetary Science Letters*, *177*(3-4), 163-176.
217 Dieterich, J. H. (1972), Time dependent friction in rocks. *Journal of Geophysical*
218 *Research*, *77*, 3690-3697.
219 Dieterich, J. H. (1978), Time dependent friction and the mechanics of stick-slip. *Pure*
220 *and Applied Geophysics*, *116*(4-5), 790-806.

221 Dieterich, J. H. (1979), Modeling of rock friction. 1. Experimental results and
222 constitutive equations, *Journal of Geophysical Research*, *84*(NB5), 2161-2168.
223 Dieterich, J. H., and B. D. Kilgore (1994), Direct observation of frictional contacts -
224 New insights for state-dependent properties, *Pure and Applied Geophysics*, *143*(1-3),
225 283-302.
226 Dysthe, D. K., et al. (2002), Universal scaling in transient creep, *Physical Review*
227 *Letters*, *89*(24), 4.
228 Foster, M. C., and G. E. Ewing (2000), Adsorption of water on the NaCl(001) surface.
229 II. An infrared study at ambient temperatures, *Journal of Chemical Physics*, *112*(15),
230 6817-6826.
231 Gratier, J.-P. (1993), Experimental pressure solution of halite by an indenter
232 technique, *Geophys. Res. Lett.*, *20*, 1647-1650.
233 Gratier, J. P., et al. (1999), How pressure solution creep and fracturing processes
234 interact in the upper crust to make it behave in both a brittle and viscous manner,
235 *Journal of Structural Geology*, *21*(8-9), 1189-1197.
236 Heslot, F., et al. (1994), Creep, stick-slip, and dry-friction dynamics - Experiments
237 and a heuristic model, *Physical Review E*, *49*(6), 4973-4988.
238 Karcz, Z., et al. (2006), Stability of a sodium chloride indenter contact undergoing
239 pressure solution, *Geology*, *34*(1), 61-63.
240 Marone, C., et al. (1990), Frictional behavior and constitutive modeling of simulated
241 fault gouge, *Journal of Geophysical Research-Solid Earth and Planets*, *95*(B5), 7007-
242 7025.
243 Marone, C. (1998), Laboratory-derived friction laws and their application to seismic
244 faulting, *Annual Review of Earth and Planetary Sciences*, *26*, 643-696.

245 Rice, J. R. (1983), Constitutive relations for fault slip and earthquake instabilities,
246 *Pure and Applied Geophysics*, *121*(3), 443-475.
247 Rice, J. R., and A. L. Ruina (1983), Stability of steady frictional slipping, *Journal of*
248 *Applied Mechanics-Transactions of the Asme*, *50*(2), 343-349.
249 Ruina, A. (1983), Slip instability and state variable friction laws, *Journal of*
250 *Geophysical Research*, *88*(NB12), 359-370.
251 Scholz, C. H. (1998), Earthquakes and friction laws, *Nature*, *391*(6662), 37-42.
252 Scholz, C. H. (2002), *The mechanics of Earthquake and Faulting*, 496 pp., Cambridge
253 University Press, Cambridge.
254 Shimamoto, T., and J. M. Logan (1984), Laboratory friction experiments and natural
255 earthquakes - An argument for long-term tests, *Tectonophysics*, *109*(3-4), 165-175.
256 Shimamoto, T. (1986), Transition between frictional slip and ductile flow for halite
257 shear zones at room-temperature, *Science*, *231*(4739), 711-714.
258 Voisin, C., et al. (2002), Process and signature of initiation on a finite fault system: a
259 spectral approach, *Geophysical Journal International*, *148*(1), 120-131.
260

261 **Figure captions**

262 **Figure 1.** Schematic representation of the friction experiment. The 1 cm^2 surface area
263 salt sample is housed in a plate made of a nickel iron alloy (Invar©) to limit thermal
264 perturbations. A constant continuous velocity is imposed on the plate through a
265 brushless motor. The maximum amount of slip is limited to 1.6 cm. The loading
266 velocity can be reversed in order to achieve larger displacements. The frictional
267 behaviour as well as its overall evolution is not affected when operating this way.
268

Figure 2: (**A**) Change in frictional behavior of a salt/glass friction experiment (loading velocity: 0.11 µm/s; normal load: 0.26 MPa). The slider exhibits regular stick-slip at the beginning with a jump amplitude of about 35 µm and a waiting time of about 300 s. At the end of the experiment, the slider exhibits an episodic stable sliding behavior with small oscillations of its speed around the imposed velocity. Color insets represent the topography of the frictional interface before and after the experiment measured by white light interferometry, with a roughness resolution of 0.05 µm (Wyko 2000 Surface Profiler from Veeco). Column **(B)** stands for the beginning of the experiment. The accumulated slip is about 500 µm. The stick-slip behavior is clearly recorded both in horizontal and vertical displacements. Amplitudes are of the order of 20 µm and 0.3 µm in horizontal and vertical directions respectively. Long phases of stress build-up are followed by rapid force drops of up to 3 N as the slider moves abruptly. Column **(C)** stands for the mid-run of the experiment, with a cumulated slip of 2500 µm. The stick-slip behavior is still recorded. Horizontal and vertical jumps are visible with amplitudes of about 10 µm and 0.1 µm respectively. The stress drops are about 2 N. Column **(D)** stands for the end of the experiment, with a cumulated displacement of about 6000 µm. Smooth oscillations typical of the episodic stable sliding regime are recorded. Note that the mean force that has to be exerted for the slider to move has increased: the friction coefficient has increased and the contact interface has strengthened. This is consistent with the increase of the real area of contact.

Figure 3. (A) Stick-slip amplitude (Δd) versus waiting time (Δt) for the friction experiment PUSH057. Color codes for increasing time: magenta; blue; red; yellow; and black. A clear trend to a decrease in amplitude and waiting time arises from the data. All control parameters being constant, the spreading of data characterizes the

morphological change of the interface. The red star (left lower corner) indicates the final state to be reached by the slider: the slider moves at the exact imposed velocity. The inset shows the settlement of the slider during the experiment, consistent with the PSC deformation of the interface. Second-order oscillations corresponding to stick-slip events also decrease with time. **(B)** Velocity jump experiments for a, b and d_c estimates. The slider is submitted to velocity cycles (1 and 10 µm/s). The black rectangles indicate the periods of slow velocity. The three lines correspond to three exerts of an experiment (constant conditions of normal stress and temperature – no gouge development) taken at different times and cumulated displacement. Sudden drops in friction observed at 1.53 and 4.5 cm corresponds to change in the direction of slip. Line 1: the direct friction effect (related to a) and the slow relaxation (related to b) are visible. Estimates of a, b and d_c are: 0.1209±0.0094, 0.26±0.0296 and 22.33±5.86 µm respectively. Line 2: the direct friction effect has disappeared. Estimates of a and d_c following the methodology of *Dieterich and Kilgore* [1994] are not appropriate. The change in velocity induces an immediate change in friction (b = 0.0862±0.0252) that is also decreasing in amplitude with the cumulated displacement. Line 3: the change in friction is no more visible. The slider has become velocity neutral.

Figure 1

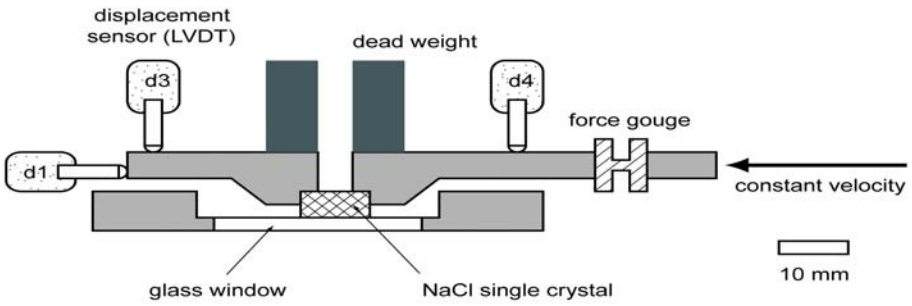

315 Figure 2

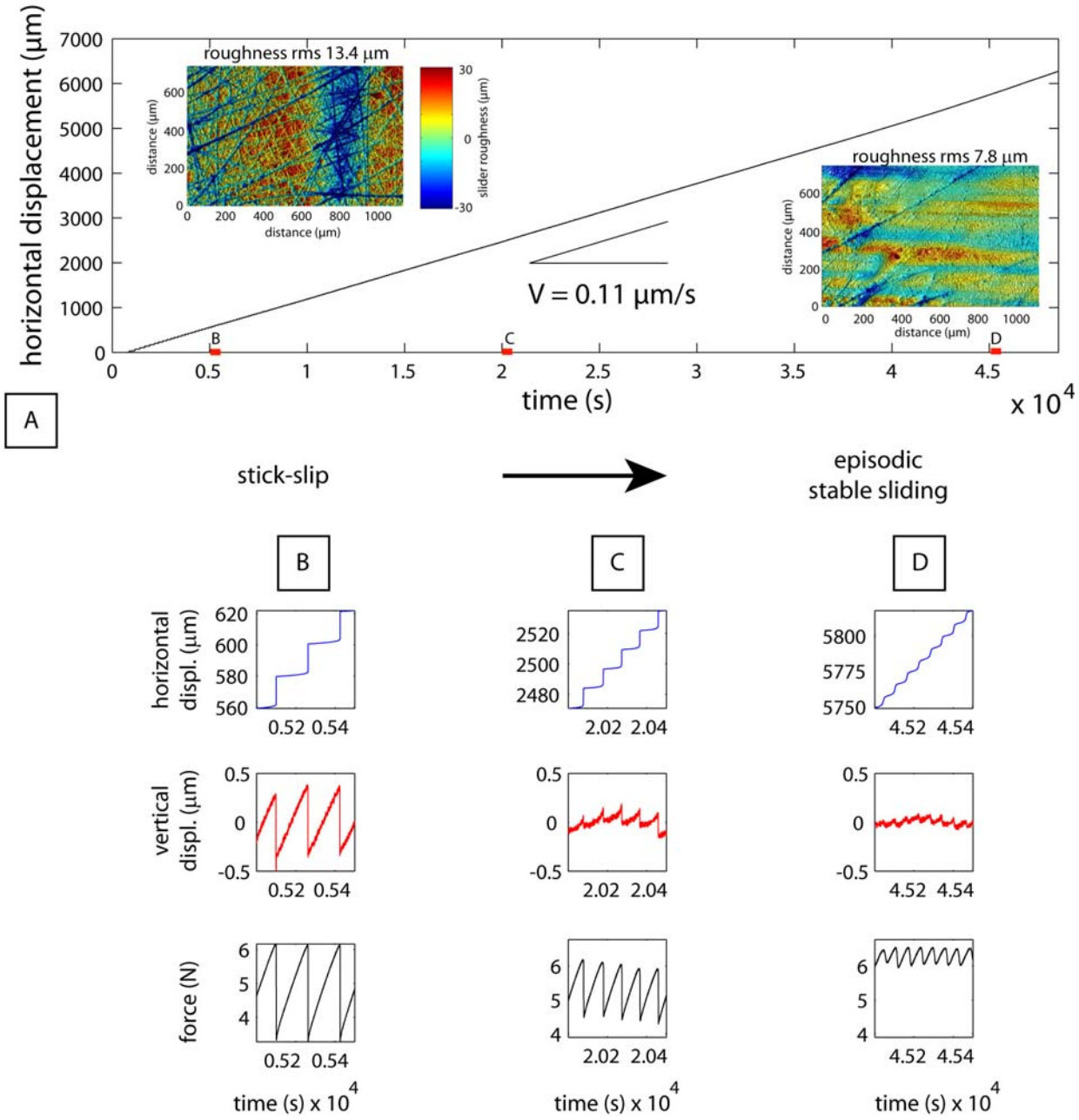

316
317
318

319 Figure 3

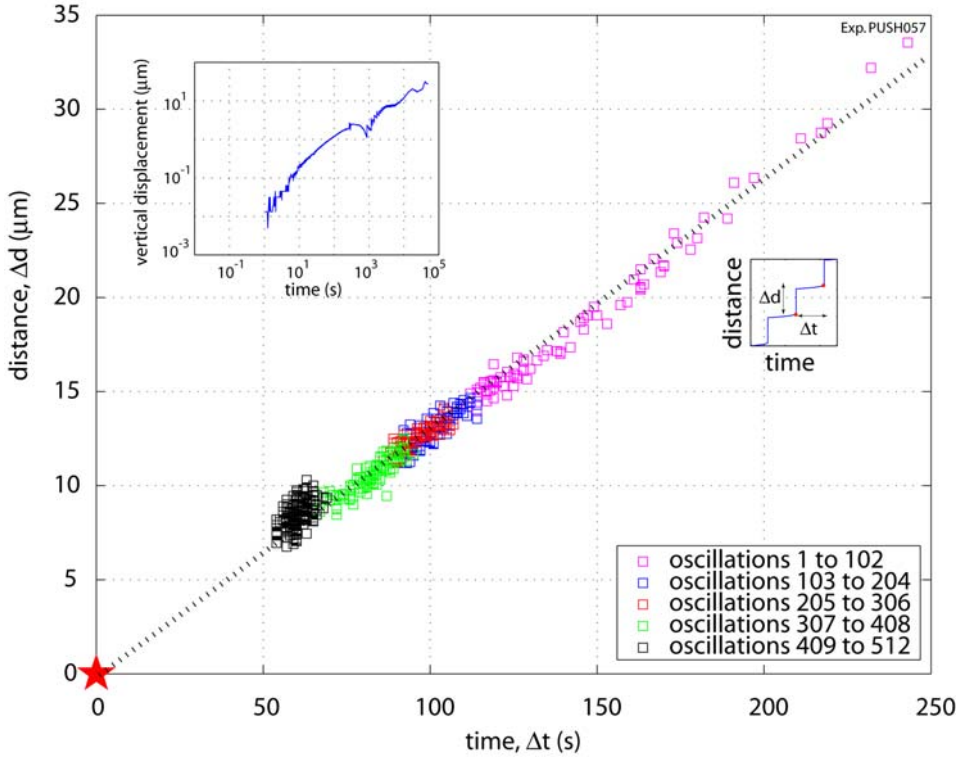

320
321 A

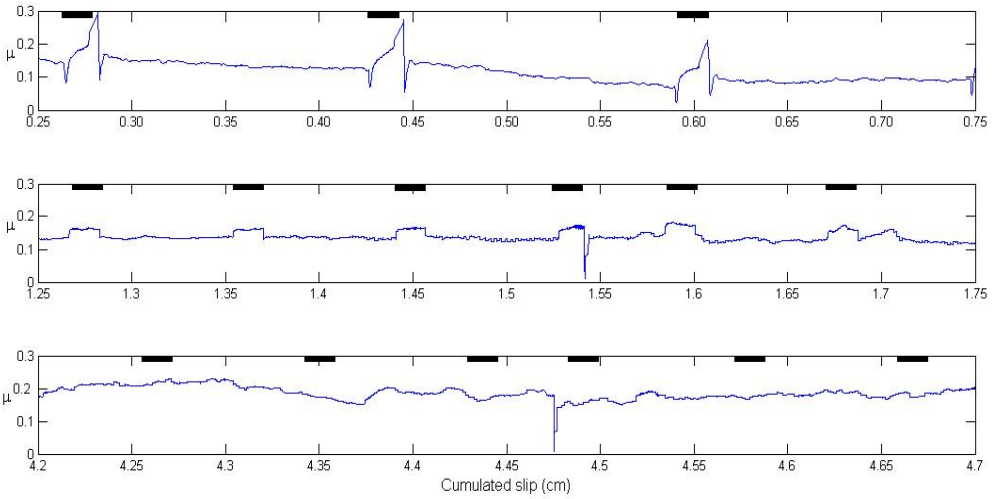

322
323 B